Research on online detection System of lathe tool wear based on Machine Vision

Yufeng Ding
Wuhan University of Technology
Pucheng Wan (1848545939@qq.com)
Wuhan University of Technology
Bo Zhang
Wuhan University of Technology

Research Article

Keywords: Tool wear, Machine vision, Online detection, Image processing

Posted Date: March 22nd, 2021

DOI: https://doi.org/10.21203/rs.3.rs-335810/v1

Research on online detection System of lathe tool wear based on Machine Vision

Ding Yufeng Wan Pucheng Zhang Bo

School of mechanical and electrical engineering, Wuhan University of Technology

(Wuhan, China, 430070)

Email: pucheng_wan@163.com

Abstract: Machine tools are important factor to determine the surface quality of the workpiece, and the online detection of tool wear is of great significance to the production and processing. In this paper, turning tools are taken as the research object, the tool wear evaluation index is defined, and the online detection system of lathe tool wear based on machine vision is designed. The workpiece processing, tool wear image acquisition, transmission, storage, and processing are completed in this system. Aiming at the problem of tool wear state detection, an adaptive hybrid filtering method is proposed in order to remove noise in the image acquisition process, nonlinear transformation and unsharp masking methods are used to enhance tool wear image quality. The GrabCut improved algorithm is used to segment the tool wear image. The Canny edge detection operator with adaptive double thresholds is used to detect the edge of the tool wear area. Finally, the upper and lower boundaries of the tool wear area are detected by using the Hough transform method, and the wear value of the tool flank is calculated, which is compared with the blunt standard $VB = 0.6mm$ to determine whether the tool needs to be replaced. The accuracy of the detection method is verified by experimental measurement of the surface roughness of the workpiece after machining.

keywords：Introduction

The traditional tool wear state detection needs to be judged by experience, or by shutdown measurement. This method is subjective, easy to misjudge, and requires high ability of workers, which is difficult to meet the requirements of intelligent manufacturing.

Tool wear detection methods are divided into two types: direct measurement method and indirect measurement method. The indirect measurement method determines the wear state of machine tools by measuring the cutting force during the machining process, the cutting temperature generated by cutting, machine tool vibration

and noise and other processing information. They are studied by various researchers[1-4]. Although it allows to monitor the tool condition in real time, it is connected with cutting parameters and complicated to deal with.

The common method for tool wear detection is to detect the tool wear state of machine tools by measuring the cutting force, cutting temperature generated by cutting, machine vibration, and noise in the machining process. Since this information cannot strictly correspond to the tool wear, and the installation of sensors is inconvenient, it is easy to be affected by the machining conditions and environment, so there are certain limitations.

The tool wear detection method based on machine vision is a direct measurement method. It uses image processing algorithm to process and analyze the collected tool wear image, and extracts the wear value of the tool wear image, and compare it with the tool blunt standard to determine the tool wear state. This method has the advantages of high detection accuracy and fast speed. Tool wear detection methods based on machine vision include tool wear detection of workpiece surface texture features, tool wear detection of workpiece chip images, and tool wear detection methods of tool knife face images. Wen-Yuh Jyw et al.[5] used machine vision to obtain the texture image of the workpiece surface, and carried out weighting calculation according to the surface texture. The experiment showed that the standard deviation of the workpiece surface texture data result can be used as an indicator of tool replacement. Zhang Peipei et al.[6] established the relationship between the width and bending radius of the workpiece chip and the tool wear value. The experiment shows that as the degree of tool wear increases, the width and bending radius of the chip gradually decrease.

In this paper, the tool wear state is measured by analyzing tool surface image. The image processing technology is used to measure the flank wear width of the tool directly, the depth of the front tooth depression, the length of the cutting edge, and the fillet radius of the tool tip. The tool wear state is judged by comparing with the tool blunt standard.

Guan Shengqi[7] used Gaussian filtering and Gaussian difference filtering to process the tool wear image. Through the center-peripheral operation between the Gaussian filter map and the Gaussian difference filter map, a significant image of tool wear was formed to achieve wear image enhancement. Peng Ruitao[8] used the CCD camera to collect the tool wear images, established wear boundaries through image preprocessing, threshold segmentation, edge detection based on Canny operator and

sub-pixels, and extracted milling machine tool wear. Qing Guohua[9] used Otsu and spline curve fitting method to enhance the contrast of wear area and background area, and realized the segmentation and calculation of tool wear area by adaptive variance threshold method and morphological description method. Liao Yusong and Han Jiang[10] used a Canny operator to detect the edge of tool wear area and used pixel distribution continuity judgment method to remove the false edge points in the edge of tool wear image, and realized the edge extraction of tool wear area. Guan Shengqi[11] carried out gray transform and wavelet single layer transform on the tool wear image to eliminate the influence of uneven illumination. The filtered tool wear image was standardized and fused. The interclass variance method was used to segment the tool wear image, and the tool wear detection was realized.

JinLin Zhang[12]proposed a machine vision-based end mill wear detection system, which extracts the edge of the tool wear area through column scanning, finds the correct edge position in each wear column, uses sub-pixel edge detection technology for edge extraction, and reconstructs the wear area Obtain the wear value of the upper and lower edges. Qiulin Hou[13]used the adaptive connection domain marking method for edge separation, and used the threshold method to extract the cutting edge and calculate the tool wear. The experiment shows that this method can quickly and effectively detect tool wear with high detection accuracy. Jamie Loizou[14] proposed a broach wear measurement method, which quantifies the wear of the broaching tool according to the total wear area, making the measurement of broach wear more accurate.

Extensive research has been conducted for the tool wear measurement method. Although they have done extensive researches about the tool wear detection based on machine vision and made great process, there is a long way to go. Few researches have been done in lathe tool field. In this paper, a lathe tool wear detection system based on machine vision is proposed.

The rest of the paper is organized as follows. Sec. 2 introduces the high-quality acquisition method of lathe tool wear images, including the selection of the camera and the key technology of the acquisition system. Tool wear image processing includes image noise reduction, image enhancement, area segmentation, edge detection, determination of tool wear boundaries, and the calculation method of tool wear value are introduced in Sec. 3. Sec.4 establishes a lathe tool wear detection system, and conducts experiments to verify the detection results by measuring the surface roughness of the workpiece. Finally, Sec. 5 summarizes the research results done in this article.

1 High quality image acquisition method of lathe tool wear

1.1 Tool wear evaluation index

When tool is worn to a certain limit, it cannot continue to be used, this wear limit is the tool blunt standard. According to ISO, on the tool flank face, the wear band width VB of 1 / 2 depth of cut is used as the blunt standard of tool. General tool grinding blunt standard [15] is shown in table 2-1. Table 2-2 is tool bluntness standards recommended by ISO[16].

Table2-1 Standard for bluntness of lathe cutters

Cutting tool type	Work material	Processing properties	Standard of abrasion VB(mm)	
			High speed steel	Cemented carbide
Straight tool	Carbon, alloy steel	Rough turning	1.5~2.0	1.0~1.4
		Finish turning	1.0	0.4~0.6
Facing tool	Gray cast iron, malleable cast iron	Rough turning	2.0~3.0	0.8~1.0
		Finish turning	1.5~2.0	0.6~0.8

Table2-2 Tool bluntness standard recommended by ISO

Standard of abrasion	Application
Destruction line damaged	High-speed steel tool
Rear face ' s wear VB=0.3mm	Cemented carbide and ceramic tools, display uniform back tool surface
Rear face ' s wear $VB_{\max}$=0.6mm	Uneven wear of the main flank face
Measurement by roughness value R_a：1、1.6、2.5、4、6.3、10 um	Subject to roughness requirements

In this paper, the hard alloy cylindrical cutter is used to finish the stainless steel 420 workpiece, and the wear of the main flank is uneven. Under the condition of meeting the roughness requirements, the wear blunt standard $VB=0.6mm$ is comprehensively considered.

1.2 High quality image acquisition technology for tool wear

The process of image acquisition generally uses the optical imaging module to image the object under the auxiliary illumination of an appropriate external light source. The position and angle of the object or the focal length of the imaging equipment are adjusted to be clear, and the image of the object is converted to digital image information, which is transmitted to the computer for image processing.

1.2.1 Camera selection

The combined portable digital microscope can collect the image of the tool with high definition, and the image is saved directly to the computer through a USB serial port. The camera parameters are shown in tables 2-6.

Table2-6 Camera parameters

Camera name	Supereyes digital microscope	Image rate	30FPS
Resolution magnification	5M 100~2000X	Working distance transmission mode	1~300mm USB serial

1.2.2 Key technology of high-quality image acquisition system

1. Imaging sharpness judgment and camera focusing setting

The definition evaluation function is an important evaluation index reflecting image definition. At present, the definition evaluation method based on image gradient information is widely used. The commonly used gradient evaluation function is to extract the edge and contour information of the image and construct the evaluation function after differential operation. The commonly used gradient evaluation functions include Sobel operator, Laplacian operator, and variance evaluation function[17].

Four different resolution tool images are given in Fig 2-1. Through C + + programming, three kinds of sharpness evaluation functions, Sobel evaluation function, Laplacian evaluation function and variance evaluation function, are used to calculate the sharpness evaluation index.

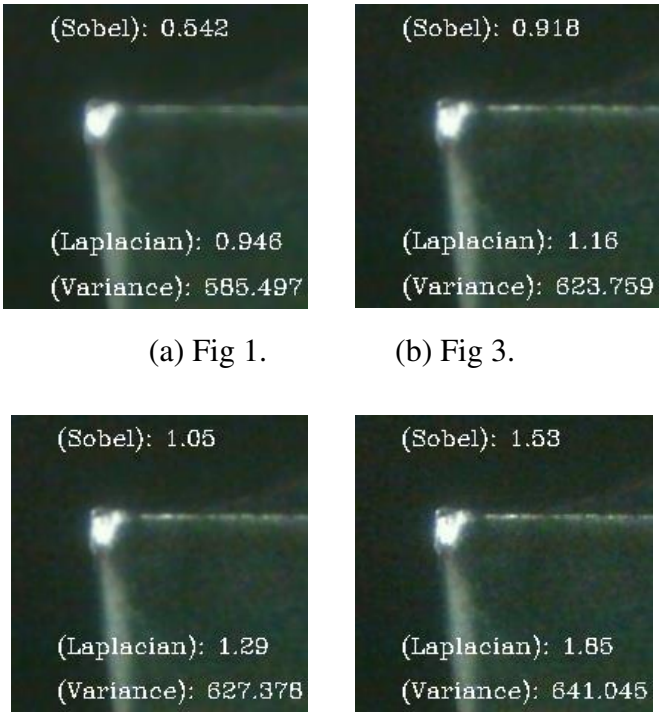

(a) Fig 1. (b) Fig 3.

(c) Fig 3. （d）Fig 4.

Figure2-1 Evaluation results using sharpness evaluation function

Table 2-3 Statistics on sharpness evaluation of four images:

Table2-3 statistics of sharpness evaluation

	Sobel evaluation function	Laplacian evaluation function	Variance evaluation function	definition
Fig 1.	0.542	0.946	585.479	minimum
Fig 2.	0.918	1.16	623.759	third
Fig 3.	1.05	1.29	627.378	second
Fig 4.	1.53	1.65	641.045	maximum

The sharpness evaluation function is that the larger the data index, the clearer the image is. The statistics of sharpness evaluation are shown in Table 2-3. Therefore, in the actual shooting of the tool image, the focus of the camera is adjusted manually to shoot the tool wear image, and the sharpness evaluation function is used to calculate the sharpness index of the image. The camera focal length is adjusted to make the sharpness index of the tool image maximum, and the camera focal length is selected to collect the tool wear image.

2. Measurement error analysis of tool wear image

There is a certain deviation between actual imaging and theoretical imaging, which is called lens distortion. Lens distortion is generally divided into three kinds, radial distortion, eccentric distortion, and thin prism distortion.

Fig 2-2 is the image of the camera calibration ruler. From the shooting results, although the center of the image is clear, the images on both sides are fuzzy, which is a common lens distortion phenomenon. The error values of the size measured by the camera software and the actual size are compared many times, and the error is within 5 %, so the lens distortion can be ignored.

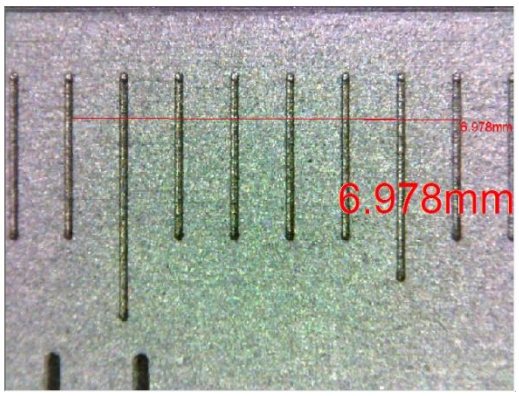

Fig2-2 Image taken by camera

3. Camera calibration

According to the imaging principle, the width of the tool flank wear area is the product of the number of pixels in the tool image and the actual size ratio of each pixel. However, the actual size of each pixel needs to be corresponding to the magnification, so it is necessary to calibrate the camera.

The camera calibration method is generally compared with the standard ruler. The specific method is to shoot the image of the standard ruler under a certain magnification and record the actual length of the ruler under the magnification as L. Then, the number of camera pixels within this length is counted as N_0. The actual size of each pixel is calculated as S_0. The calculation formula is:

$$S_0 = \frac{L}{N_0} \tag{0.1}$$

Then tool wear image is taken under the same magnification, and the number of pixels occupied by tool flank wear width is calculated as N_r, and the actual tool wear width S_r is calculated according to the formula:

$$S_r = N_r \bullet S_0 = N_r \frac{L}{N_0} \tag{0-2}$$

The actual pixel size of tool wear images at different magnifications is shown in table 2-4.

Table2-4 Pixel size of tool wear image under different magnification

Magnification	13.8	20	28	35
Actual pixel size of wear image （μm）	16.2	11.4	8.06	6.56

2 Image detection method of tool wear

Tool wear value cannot obtain directly from collected tool wear image, and the tool wear state can only be judged after image processing and analysis. The purpose of image processing is to maximize the interference in the tool wear image, highlight the characteristics of the target, simplify the target area, and improve the accuracy and speed of detection. In this paper, a complete set of image denoising, image enhancement, object segmentation and edge detection techniques are used to process the tool wear image. The image processing flow is shown in Fig 3-1.

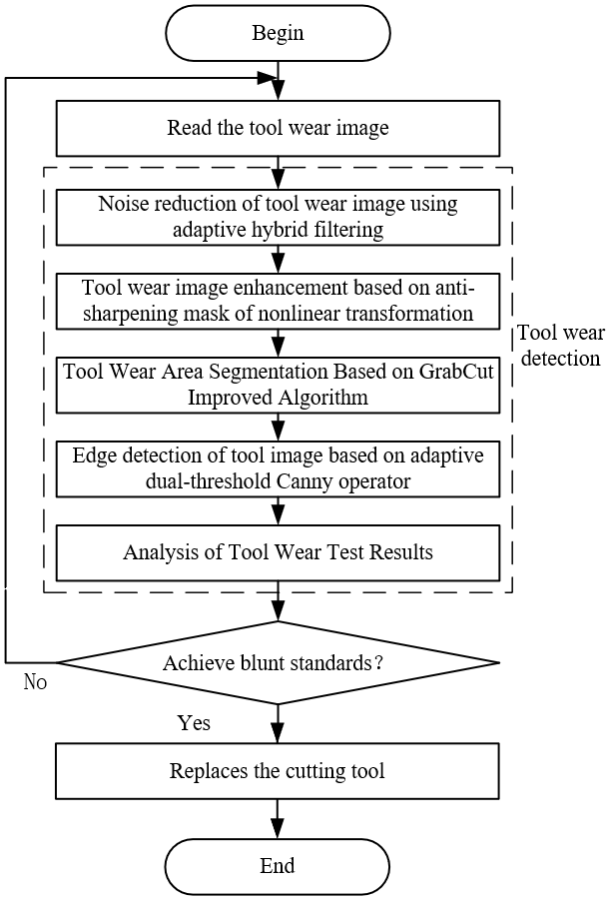

Fig 3-1 Tool wear image processing flow chart

2.1 Noise reduction of tool wear image using adaptive hybrid filtering

Due to the complexity of the workshop working environment, the collected tool image is often interfered by noise from the external environment and the internal structure of the imaging equipment. These noises can usually be divided into two categories, one is salt and pepper noise, and the other is Gaussian noise[18]. Therefore, it is necessary to denoise tool image. Median filtering is a nonlinear filtering algorithm [19]. It has an excellent filtering effect on noise interference and can protect image details. At the same time, Gaussian noise is often accompanied in the process of image acquisition and transmission, so it is necessary to use Gaussian filtering for tool image denoise.

In this paper, adaptive mixed filtering is used. Adaptive mixed filtering includes Gaussian filtering and adaptive median filtering. Adaptive median filtering can adaptively change the size of the template, which can not only ensure an excellent smoothing effect, but also ensure the edge of the image. The adaptive median filter has a window of S_{xy}, and the size of this window will change in the filtering process. The output of the filter is a pixel value, and an intermediate value (x, y) is used to replace the value of the window center.

The adaptive hybrid filtering process is shown in Fig 3-2.

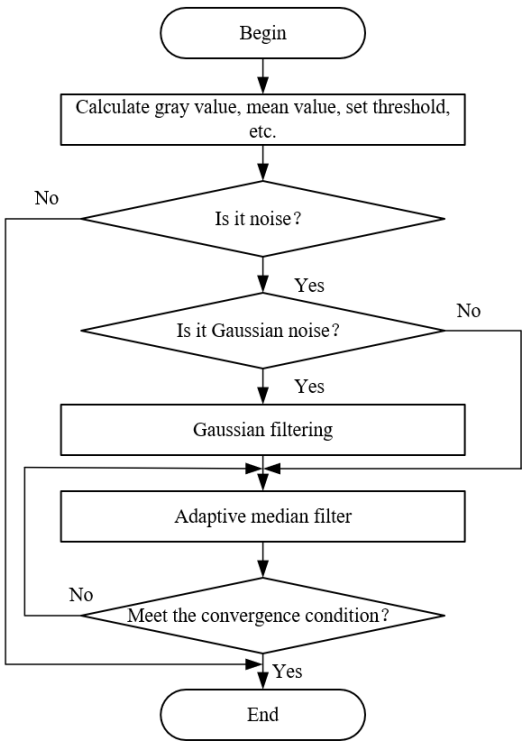

Fig 3-2 Adaptive hybrid filtering process flow chart

Gaussian filtering, median filtering, and adaptive mixed filtering are used to process the tool wear images collected in the process of machine tool processing experiment. The comparison results after filtering are shown in Fig 3-3.

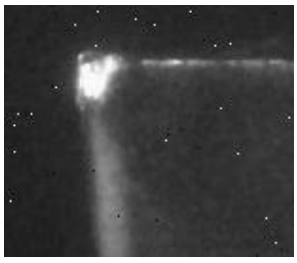

(a) Noised Image

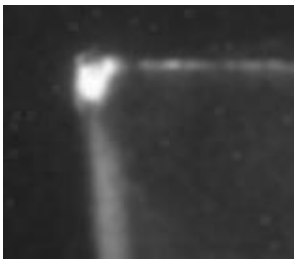

(b) Gaussian Filtering Image

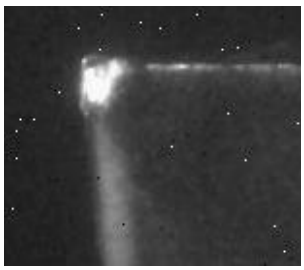

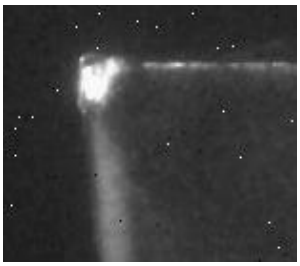

(c)3 Kernel Median Filtering Image (d) 5 Kernel Median Filtering Image

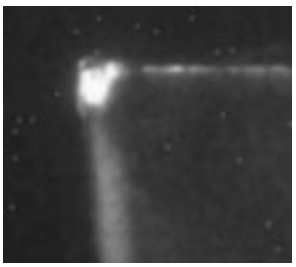

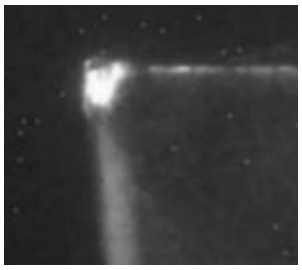

(e) Gaussian Filtering Plus Median Filtering (f) Adaptive Hybrid Filtering Image

Fig 3-3 Comparison of Gaussian Filtering, Median Filtering, and Adaptive Hybrid Filtering

From the filtering results, although Gaussian filtering has a perfect suppression effect on Gaussian noise, it cannot remove salt-pepper noise and leads to image blur. The median filter has an outstanding effect on salt-pepper noise suppression, but the median filter with a smaller kernel has an insufficient suppression effect. The median filter with a larger kernel will cause image blur and cannot suppress Gaussian noise well. Gaussian filtering combined with median filtering still has the above problems. Adaptive mixed filtering can suppress Gaussian noise and salt-pepper noise, and

adaptive median filtering can adjust the size of the template, almost no image blur, so the filtering effect is the best.

2.2 Tool wear image enhancement based on nonlinear transformation and anti-sharpening mask

After noise reduction, the tool wear image will change the gray value of the image, resulting in changes in the contrast and edge information of the image, and the image becomes blurred. To improve the overall visual effect of the image, it is necessary to enhance the tool wear image. The Gamma correction method is used.

2.2.1 Image enhancement based on Gamma and nonlinear transform

The transformation formula for Gamma correction is:

$$I_{out} = AI_{in}^{\gamma} \tag{0-3}$$

Where A is a constant and γ is a correction coefficient.

Gamma correction adjusts the contrast of the image by selecting the appropriate correction coefficient, which can be used to improve the image details and make the visual effect of the image better. Fig 3-4 shows the images under different correction coefficients and corresponding grayscale images.

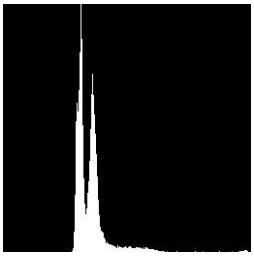

(a) γ=1 gray histogram

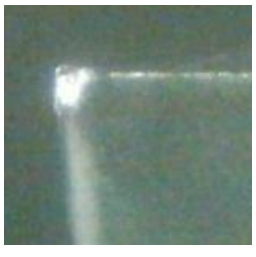

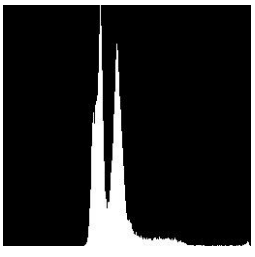

(b) γ=0.5 gray histogram

(c) γ =0.1 gray histogram

Fig 3-4 Images and corresponding gray histograms under different Gamma correction coefficients

Gamma correction can greatly enhance the low gray value of the region, which greatly improves the details of the image. However, brightness of some areas of the image are too strong, not conducive to further image processing.

In order to suppress some high-brightness regions, strengthen the low-brightness part, and enhance the image balance, the nonlinear transformation is adopted for the image. The definition of nonlinear transformation is:

$$I_1(x,y) = (\frac{2}{1+e^{-m}} - 1) \times 255 - v(x,y) \tag{0-4}$$

$$m = k(v) \times \frac{v}{v + a\bar{v}} \tag{0-5}$$

$$k(v) = \begin{cases} A & (0 \le v \le A_1) \\ \dfrac{v - A_1}{B} & (A_1 \le v \le B_1) \\ \dfrac{v - B_1}{C} & (B_1 \le v \le C_1) \end{cases} \tag{0-6}$$

Among them, $v(x,y)$ is the gray value of (x,y) point in the image, a is the adjustment coefficient, $\bar{v}$ is the average gray value of the image, A, B and C are constants between 0 and 255, A_1, B_1 and C_1 are gray value thresholds. Nonlinear transformation can suppress high light very well. Since the average gray value of the image is considered by the non-linear transformation, the non-linear transformation has an excellent adjustability, can adapt to the situation that the gray value of the image changes violently, and has an outstanding enhancement effect on the image. Fig 3-5 shows the effect of image suppression after the original image and nonlinear transformation.

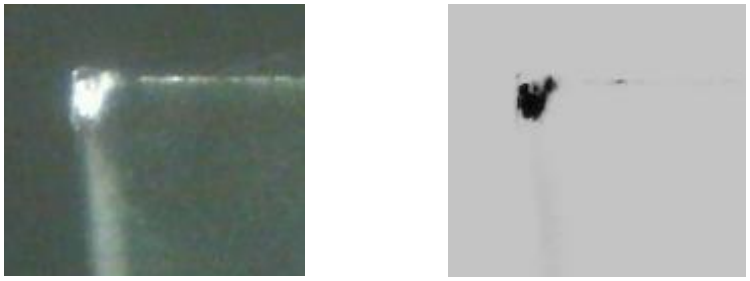

(a) original image (b) nonlinear transformation image

Fig 3-5 Original image and results of image suppression after nonlinear transformation

The brighter part of the original image in Fig 3-5 corresponds to the darker part of the right-hand nonlinear transformation image. After nonlinear transformation, the contrast of the image is adjusted well, the high brightness region is partially suppressed, and the low brightness region is improved to some extent. Finally, Gamma correction image, nonlinear transformation, and the original image are synthesized as follows.

$$I = k_1 I_{out} + k_2 I_1 + k_3 I_0 \tag{0-7}$$

After synthesis, since the gray value exists between 0 and 255, it needs to be normalized, and the final gray value is processed by the adaptive standard deviation truncation method. Fig 3-6 shows the images synthesized by the Gamma correction image, nonlinear transformation, and the original image. After comprehensive treatment, the brightness area of the image has been suppressed to some extent, and the dark area has been enhanced, and the texture feature of the image has been well preserved.

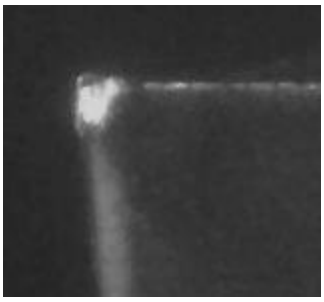

Fig 3-6 Gamma correction, nonlinear transformation and original image synthesis results

2.2.2 Image detail enhancement based on anti-sharp masking algorithm

After the image contrast compression by using Gamma correction and nonlinear transformation, the texture feature of the image is enhanced better than the original image. To obtain better tool wear boundaries and provide conditions for the edge detection of tool wear area, the anti-sharp masking filtering algorithm is used to enhance the image details. The purpose is to improve the high-frequency components in the image and enhance effectively the contour of the tool wear image.

The mathematical expression of the anti-sharp masking algorithm is:

$$G(x,y) = f(x,y) + k \times (f(x,y) - g(x,y)) \tag{0-8}$$

where $G(x,y)$ is the transformed image, $f(x,y)$ is the original image, $g(x,y)$ is the image with fuzzy details in the process of image processing, and k is the weight factor. By adjusting the weight factor, different image enhancement effects can be obtained, the outline of the image is more clear. Fig 3-7 shows the image processed by the anti-sharp masking algorithm.

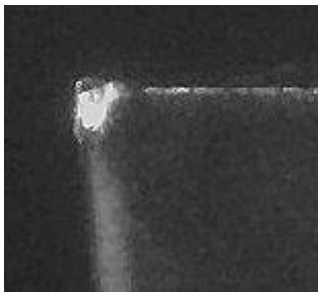

Fig 3-7 Result image processed by anti-sharp masking algorithm

2.3 Tool wear region segmentation based on GrabCut improved algorithm

After the image is denoised and enhanced, the tool wear area needs to be segmented for tool wear edge detection. Traditional image segmentation methods include a threshold-based segmentation method, an edge-based segmentation method, a region-based segmentation method, and a graph-based segmentation method [20]. GrabCut algorithm is based on the graph theory combination optimization method, and the segmentation effect is better. The process of the GrabCut algorithm segmentation image is shown in Fig 3-8.

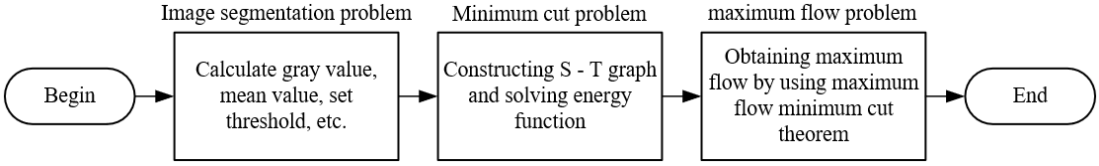

Fig 3-8 The process of image segmentation by GrabCut algorithm

The traditional GrabCut algorithm is sensitive to the initial value, and it is difficult to meet the needs of engineering. If the framed part of the image is a non-convex polygon, the algorithm will select additional information. Although redundant background can be eliminated by multiple iterations, the segmentation efficiency is reduced. The Improved K-means clustering algorithm is proposed to deal with the pre-segmentation of image[21]in order to improve the segmentation efficiency of GrabCut.

2.3.1 Improved K-means clustering algorithm

K-means clustering algorithm is used to divide samples into different classes according to the similarity of sample data, and its basic process is shown in Fig 3-9. The selection of the K value of the traditional K-means clustering algorithm depends on experience or is determined by the successive incremental method, which is too subjective or inefficient to meet the requirements. The improved K-means clustering algorithm can obtain a better clustering effect and better image pre-segmentation effect.

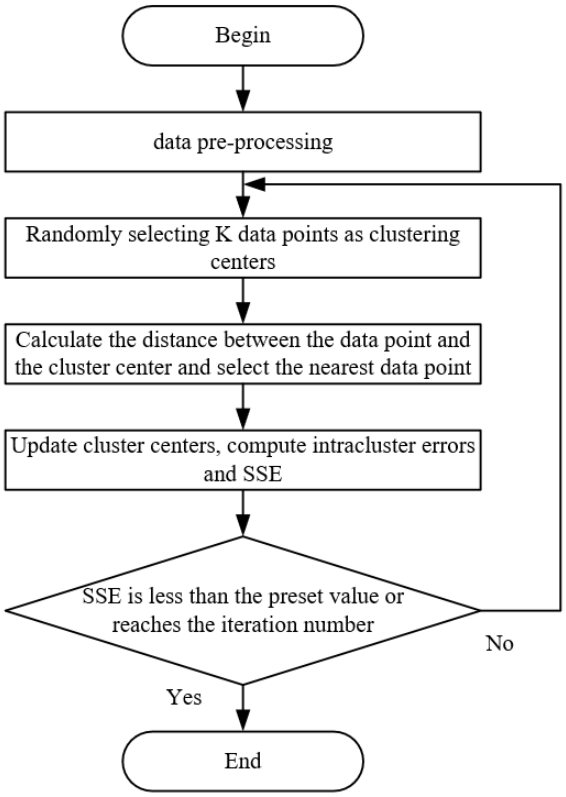

Fig 3-9 The basic process of K-means clustering algorithm

The algorithm uses the inflection point method to determine the value [22], and the outlier factor to determine the clustering center[23].

1. Optimal K value selection

By selecting different K values, the SSE (within-cluster sum of squared errors) corresponding to different K values is calculated, and the relationship curve between SSE and K is drawn, and the K value corresponding to the curve ' inflection point ' is found. The inflection point is determined by the slope of the curve. As the number of data points in the cluster center increases, similarity sample data gather together, and the variance of the data in the same cluster is getting smaller and smaller. According to the relationship curve between SSE and K value, when the K value increases to a certain extent, the slope of the sample changes sharply. This sharp change point is called the inflection point.

2. Determination of cluster centers by outlier factor optimization algorithm

Clustering algorithm divides the same class or similar objects into the same cluster. The data in the same cluster are as similar as possible, and the difference between different clusters is as large as possible. In the same cluster, the cluster center with more data points and the outlier with less data points. For outliers, try to avoid such data as the initial cluster center.

The meaning of outliers is shown in Fig 3-10. Data points with similar characteristics will gather in a certain area and form clusters, such as C_1 and C_2, and data points without similar characteristics will be far away and form isolated points, such as D_1 and D_2.

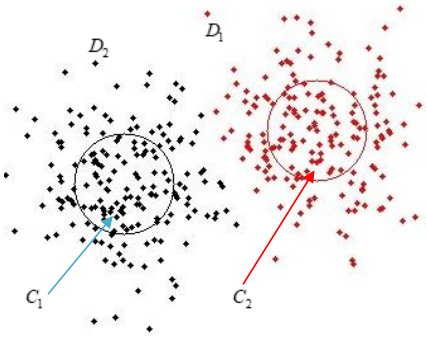

Fig 3-10 Clusters and isolated points

The goal of the outlier factor algorithm is to calculate the outlier factor of each data point, arrange the data according to the outlier factor, and select the data with the furthest distance as the initial clustering center.

By Comparing with the traditional K-means clustering algorithm, the improved K-means clustering algorithm has a better clustering effect. It lays the foundation for the image segmentation method which integrates K-means clustering algorithm and GrabCut algorithm.

2.3.2 Tool wear region segmentation based on GrabCut improved algorithm

The image processed by the improved K-means clustering method is used as the input of the GrabCut segmentation algorithm[24]. The clustering method is used to mark the wear area, and then the GrabCut algorithm is used for segmentation. It can reduce manual interaction and improve the efficiency and accuracy of tool wear image segmentation.

1. Image segmentation process based on GrabCut improved algorithm

The flow chart of image segmentation based on the improved GrabCut algorithm is shown in Fig 3-11.

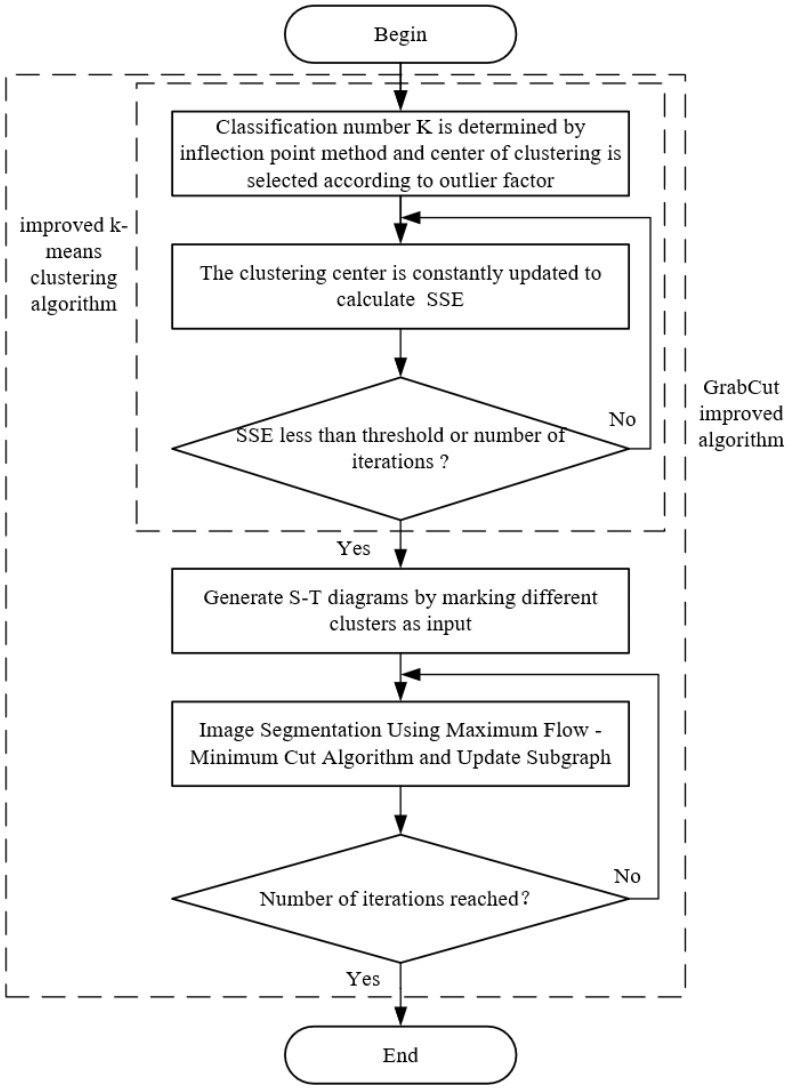

Fig 3-11 Image segmentation process based on GrabCut improved algorithm

2. Determination of classification K value by inflection point method

By calculating SSE corresponding to different K values, and the relationship curve between SSE and K value can be obtained. It is shown in Fig 3-12. According to the inflection point inflexion method, the slope of the K value decreases sharply from 1 to 2, and then the slope tends to be stable. Therefore, the point with the K = 2 is called the inflection point, and then the K = 2.

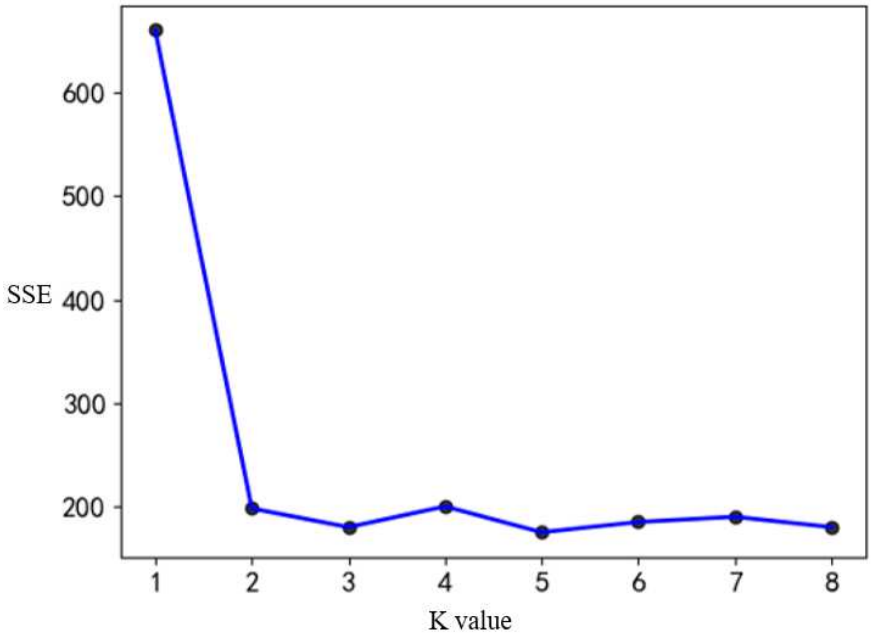

Fig 3-12 The relationship between K value and SSE

The traditional GrabCut segmentation result is shown in Fig 3-13

Fig 3-13 Traditional GrabCut segmentation result

The segmentation result of GrabCut improved algorithm under different values are shown in Fig 3-14.

(a)K=2 clustering results segmented result (b)K=3 clustering results segmented result

(c)K=5 clustering results segmented result

Fig 3-14 Segmentation results of GrabCut improved algorithm

The accuracy and recall are used to evaluate the segmentation accuracy.

$$\Pr ecision = \frac{TP}{TP + FP} \tag{0-9}$$

$$\mathrm{Re}\, call = \frac{TP}{TP + FN} \tag{0-10}$$

Where TP (True Positive) is the correct pixel in the segmentation result, FN (False Negative) is the missing pixel in the segmentation result, and FP (False Positive) is the wrong pixel in the segmentation result. The accuracy and recall of the traditional GrabCut algorithm and our algorithm are shown in Table 3-1.

Table3-1 Accuracy and recall rate of two segmentation algorithms

Algorithm comparison		Precision	Recall
Traditional GrabCut algorithm		0.85	0.89
Proposed algorithm	K=2	0.97	0.96
	K=3	0.95	0.87
	K=5	0.80	0.84

The accuracy and recall rate of the traditional GrabCut segmentation algorithm are low, and some non-wear areas are divided into wear areas, which cannot segment the tool wear area completely and accurately. It also requires manual interaction and has low efficiency. The improved GrabCut algorithm uses a clustering algorithm to classify foreground and background, and takes the classification results as the input of the GrabCut algorithm without manual interaction. When K = 2, the accuracy and recall of our algorithm has high accuracy and recall, and has a perfect segmentation accuracy.

2.4 Edge detection of tool image based on adaptive dual-threshold Canny operator

After the image is segmented, the gray level of pixels in the tool wear area and image background area has a step change, and the wear boundaries is obtained by the image edge detection method. Edge is a extremely important feature of the image, and it is one of the most important information to distinguish the target area and the

background area. In the process of tool wear detection, it is greatly important to obtain complete edge information, which is the prerequisite for accurate calculation of tool wear value.

The detection process of Canny edge detection operator is shown in Fig 3-16.

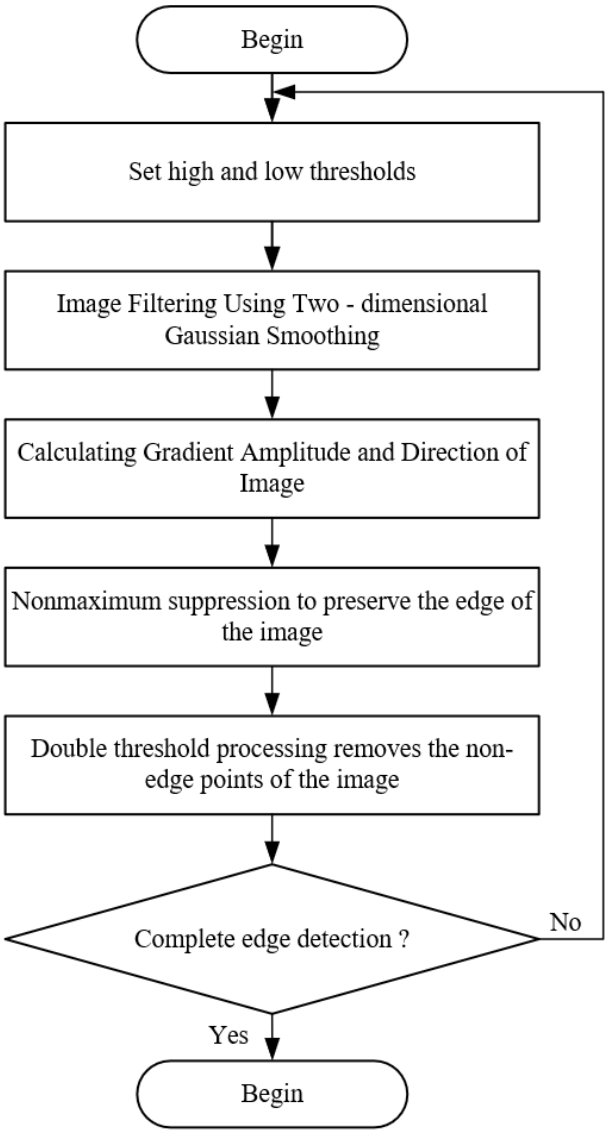

Fig 3-16 Canny edge detection process flow chart

The double thresholds T_1 and T_2 in the traditional Canny edge detection operator needs to be set manually, which has strong subjectivity and poor adaptability[25]. An adaptive threshold Canny edge detection algorithm is proposed, which can automatically select the appropriate double thresholds to achieve the purpose of automatic image edge detection.

The Otsu algorithm (Otsu) is adaptive threshold selection method. The algorithm makes the image have the best separation by selecting the optimal threshold. However, in the Otsu method, it is easy to filter out some small edges in the process of calculating

the mean value. An improved method is used which can use the gradient variance to reflect these details. The implementation process is:

（1）Calculation of gray level probability $f(x,y)$ denotes as the gray value of point (x,y) on the image. The gray level of the point on the image is distributed between 0 and L. The image size is $M \times N$, and the number of pixels S with gray level $i(i \in [0,L])$ is:

$$S = \sum_{f(x,y)=i} f(x,y) \tag{0-11}$$

Then the probability $p(i)$ of the appearance of a pixel with a gray level of i in pixels is:

$$p(i) = \frac{1}{M \times N} \sum_{f(x,y)=i} f(x,y) \tag{0-12}$$

（2）Calculation of inter class variances By selecting a reasonable threshold k, the pixels in the image is divided into two part, the target region O and the background region B, then these values can be calculated:

$$\begin{cases} P_O(k) = \sum_{i \in O} p(i) \\ N_O(k) = M \times N \times P_O(k) \\ P_B(k) = \sum_{i \in B} p(i) \\ N_B(k) = M \times N \times P_B(k) \\ g_O(k) = \sum_{i \in O} \frac{ip(i)}{P_O(k)} \\ g_B(k) = \sum_{i \in B} \frac{ip(i)}{P_B(k)} \\ \mathrm{g} = P_O(k) g_O(k) + P_B(k) g_B(k) \end{cases} \tag{0-13}$$

where $P_O(k)$ is the probability of occurrence of region O, $N_O(k)$ is the number of occurrences of region O, $P_B(k)$ is the probability of occurrence of region B, $N_B(k)$ is the number of occurrences of region B, $g_O(k)$ is the mean value of gray level of region O, $g_B(k)$ is the mean value of gray level of region B, and g is the mean value of gray level of the whole image.

The formula of Otsu algorithm to find the optimal threshold of an image is:

$$\mathrm{T} = \mathrm{Arg}Max\left[P_O(k)\left(g_O(k) - g\right)^2 + P_B(k)\left(g_B(k) - g\right)^2 \right] \tag{0-14}$$

（3）Calculation of optimal threshold k Since the between-class variance is a function of threshold value K, the maximum between-class variance can be determined according to the threshold value K. In the Otsu method, it is easy to filter out some

small edges in the process of averaging. The gradient variance can be used to reflect these details. The optimal threshold can be expressed as the gradient variance:

$$\mathrm{T} = \mathrm{Arg}\sum Max\left[P_O(k)\left(\sigma_o^2(t)-\sigma^2\right)^2 + P_B(k)\left(\sigma_1^2(t)-\sigma^2\right)^2 \right] \tag{0-15}$$

among them

$$\sigma_o^2(t) = \frac{1}{P_O(k)}\sum_{i\in O}\left(i-g_O(k)\right)^2 p(i) \tag{0-16}$$

$$\sigma_1^2(t) = \frac{1}{g_B(k)}\sum_{i\in B}\left(i-g_B(k)\right)^2 p(i) \tag{0-17}$$

$$\sigma^2 = \frac{1}{p(i)}\sum_{i\in L}\left(i-g\right)^2 p(i) \tag{0-18}$$

The highest threshold value K_2 can be obtained by the above formula, and the lowest threshold value $K_1 = 0.4K_2$ can be obtained by the estimation formula of Canny operator. After two high and low thresholds K_1 and K_2 are determined, the image is divided into three regions A_0, A_1 and A_2, which are expressed as:

$$\begin{cases} A_0 = \{(x,y), 0 \le G(x,y) \le K_1\} \\ A_1 = \{(x,y), K_1 \le G(x,y) \le K_2\} \\ A_2 = \{(x,y), K_2 \le G(x,y) \le 255\} \end{cases} \tag{0-19}$$

In the formula, region A_2 is identified as the edge of the image, region A_0 is identified as the non-edge region of the image, which will be discarded, and region A_1 is those points to be determined. If these points can be connected to the edge, they can be retained, otherwise they will be discarded.

The process of Canny edge detection operator based on adaptive double threshold is:

step1 Smooth the image and calculate the gradient vector by using the two-dimensional Gaussian function.

step2 Calculate the amplitude and direction of the image gradient.

step3 Non-maximum suppression is performed to retain the edge of the image and suppress the false edge of the image.

step4 Divide the gray level and calculate the gray level probability of each point in the image.

step5 Calculate the between-class variance, the probability $p(i)$ of gradient i, the probability of all edge points and non-edge points, the corresponding average gradient, and the average gradient of image pixel.

step6 According to the calculation formula, the gradient variance between the edge point and the non-edge point and the average gradient variance of all points are calculated. The high threshold value K_1 is selected according to the principle of maximum variance, and the low threshold value K_2 is calculated according to the formula.

The edge of tool wear image is detected by Canny operator based on adaptive double threshold, and is compared with the traditional Canny, Sobel and Laplace operators. The detection results are shown in Fig 3-17.

(a) Canny edge detector (b) Sobel algorithm (c) Laplace operator (d) Canny operator adapting to double thresholds

Fig 3-17 Comparison of edge detection operator results

Although Sobel and Laplace can detect the wear edge, it is prone to false edges, which is more chaotic and does not meet the need. Canny edge detection is not stable because the double threshold needs to be set artificially. The Canny operator based on an adaptive double threshold can automatically detect the threshold, and the non-maximum suppression is used for smoothing. It can filter out the false edge and preserve the edge well, and detect the complete edge.

2.5 Determination of tool wear boundaries by Hough transform curve fitting

After detecting the complete edge of the tool wear area, it is necessary to accurately locate the upper and lower boundaries of the tool wear area. Using the boundary distance, the tool wear value can be calculated according to the pixel value of the upper and lower boundaries of the wear area based on the camera calibration results. Hough transform is one of the commonly used methods for processing geometric shapes of planar images, which is widely used in machine vision and image processing [26].

The Hough transform is ultimately to detect the number of intersecting curves corresponding to each point in the image. If the number exceeds the set threshold, it can be considered that the intersection corresponds to a straight line on the image. The linear detection steps of the transform are as follows:

（1）In the parameter space $H(\rho,\theta)$, ρ represents the distance from the pole to the straight line, and θ is the angle between the straight line and the polar coordinate. Divide the parameter space into $m*n$ units, where ρ is divided into m equal parts, θ is divided into n equal parts, and set the accumulator $Q(\rho_m,\theta_n)$ for each unit and set it to 0;

（2）For each point (x, y) on the image boundaries, ρ corresponding to each θ is calculated according to the linear polar coordinate equation, and the corresponding unit of (ρ,θ) is found out, and the corresponding accumulator $Q(\rho_m,\theta_n)$ is accumulated by 1 ;

（3）After traversing the whole image, the value of the accumulator in each unit is counted. The (ρ_m,θ_n) corresponding to the median value of the accumulator is the parameter in the linear polar equation.

After Hough transform processing, the obtained figures are shown in Fig 3-20. The upper and lower boundaries of the tool wear region can be effectively detected. The length of the upper and lower boundaries of the tool wear image is 25 pixels. According to the camera calibration results, each pixel represents $11.4\mu m$, so the tool wear value is $0.285mm$.

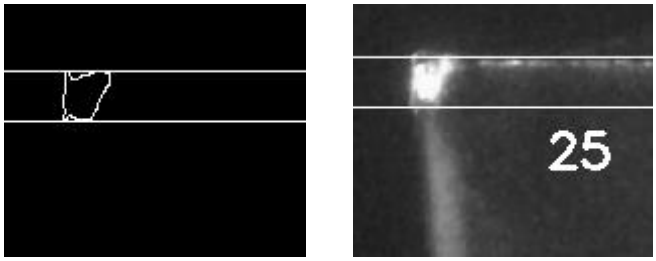

(a) Hough transform results (b) The upper and lower boundaries pixel values of the wear region

3 Fig 3-20 Hough transform detection results Tool wear detection experiment and analysis

3.1 Establishment of experimental environment

The hardware of the lathe tool wear detection system includes a CNC lathe, image acquisition system, and computer, which mainly completes the machining process of the tool, the acquisition, transmission, and storage of the tool wear image. Software functions include tool wear image acquisition, processing and tool wear state detection.

In the actual machining process, the workpiece is fixed on the three-claw chuck and rotates with the spindle at high speed. The tool is fed horizontally on the tool holder.

The axis of the camera is perpendicular to the surface of the tool to be photographed. After each tool feed is completed, the tool returns to the specified position to collect the tool image. The experimental process of tool wear detection is as follows:

（1）After each machining , the tool is retreated to the designated location. The image acquisition system is used to collect the wear image of the tool flank, and the surface roughness of the workpiece is measured after four times cutting.

（2）After each acquisition of tool wear image, the image is transmitted and saved to the computer, and the software is used for subsequent image processing;

（3）After processing the tool wear image, the detection algorithm decides whether to change tool according to the result of tool wear detection and gives the tool change information.

The tool wear detection system for lathes is shown in Fig 4-1.

(a) Lathe machine

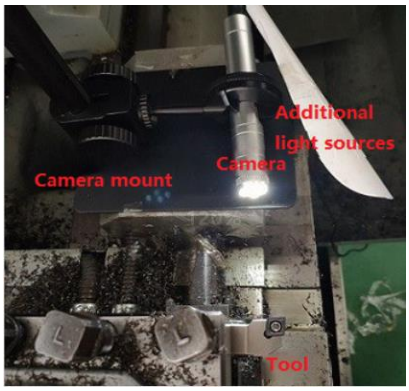

(b) Image acquisition system

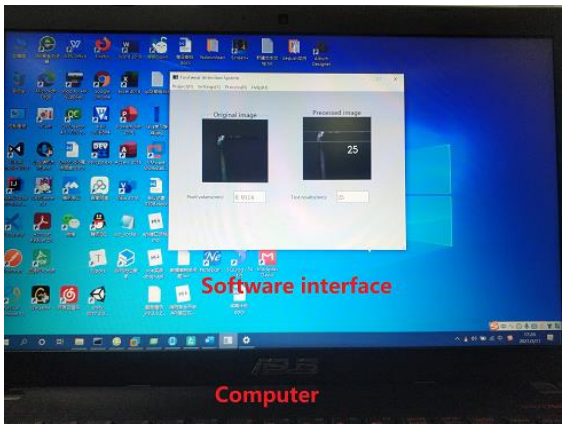

(c) Software Measuring Interface of Computer

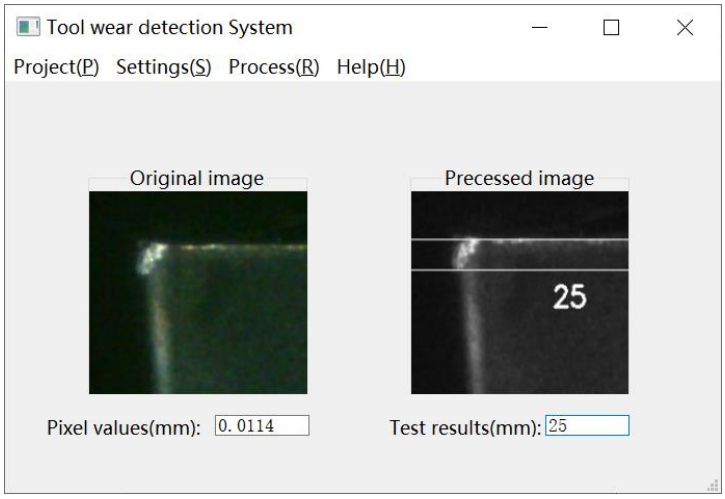

(d) Software interface

Fig 4-1 Tool wear detection system

The tool material, workpiece material, and processing parameters used in the experiment are shown in Tables 4-1.

Table 4-1 Machining Materials and Parameters

Cutter material	Hard alloy TM	Cutting depth	0.25mm
Work material	Stainless steel 420	Spindle speed	600r/min
Workpiece hardness	HRC48（heat treatment）	Feed speed	0.15mm/r
Coolant	Yes	Workpiece specification	ϕ50*150mm

3.2 Analysis of Tool Wear Test Results

The corresponding wear value is calculated by using the camera calibration results. According to the detection results of the upper and lower wear boundaries of the tool with different machining times, each pixel represents, For example, (a) in Fig 3-21. The detection value of the upper and lower wear boundaries of the tool is 12, and the tool wear value is $VB = 12*0.0114mm \approx 0.14mm$. The roughness tester is used to measure the surface roughness of the workpiece after the corresponding cutting times. The obtained tool wear image detection results are shown in Table 4-2.

Table 4-2 tool wear image detection results

Number of knife walks	Detection value (pixel)	The value of cutting-tool wear (mm)	Result of survey	Roughness (μm)

32 strikes	12	0.14	initial wear	within 1.100
88 strikes	22	0.25	normal wear	within 1.276
160 strikes	25	0.29	normal wear	
240 strikes	59	0.67	late wear	within 1.489

According to the blunt standard $VB_{\max} = 0.6mm$, the detection value of tool wear is not more than $0.6mm$. Therefore, when the tool is used to process 240 times, the tool wear value exceeds the blunt standard. At this time, although the surface roughness of the workpiece meets the surface quality requirements of $1.6\mu m$, the tool state is in the later stage of wear. The tool wear is relatively fast. Continue processing, the surface roughness of the workpiece may exceed $1.6\mu m$, which will lead to the scrap of the workpiece and not meet the processing requirements. Therefore, the tool is replaced in time before 240 times processing.

4 Summary

Tool wear on-line detection is a key technology to realize intelligent manufacturing. To solve this problem, an on-line detection scheme of lathe tool wear is designed. Aiming at the problem of image contrast reduction and blur caused by image noise reduction, nonlinear transformation, and anti-sharp masking methods are used to enhance wear image quality. A comprehensive improved K-means clustering algorithm and GrabCut algorithm for tool wear region segmentation technology is proposed, which can effectively improve the accuracy of image segmentation and reduce manual interaction. An edge detection algorithm of tool wear image based on adaptive double threshold Canny operator is proposed and applied. The algorithm has a edge detection effect, and the upper and lower boundaries of tool wear area can be extracted well by using the Hough transform curve. Taking Huazhong CNC lathe CK6136 as the experimental platform, the wear state of the lathe tool is detected by using the online detection system of lathe tool wear based on machine vision technology. The experimental results show that when the tool is processed 240 times, it exceeds the blunt standard, and the tool needs to be replaced in time.

Declarations

-Funding (information that explains whether and by whom the research was supported)
This study received financial support from National Natural Science Foundation of China (E51875429): Research on the theory and method of product manufacturing quality control in cloud manufacturing environment.

-Conflicts of interest/Competing interests (include appropriate disclosures)
The authors declare there is no conflicts of interest regarding the publication of this paper.

-Availability of data and material (data transparency)
The datasets used or analyzed during the current study are available from the corresponding author on reasonable request.

-Code availability (software application or custom code)
Some models and code generated or used during the study are proprietary or confidential in nature and may only be used with restrictions (For example, the code can run by calling Opencv Library).

-Authors' contributions (optional: please review the submission guidelines from the journal whether statements are mandatory)
Yufeng Ding. Wuhan University of Technology School of Mechanical and Electrical Engineering. Associate professor.
Ding Yufeng has put forword the wear detection method of lathe tool and software framework.
Pucheng Wan. Wuhan University of Technology School of Mechanical and Electrical Engineering. Master.
Pucheng Wan builds the image processing method of tool wear and detects the wear value.
Bo Zhang. Wuhan University of Technology School of Mechanical and Electrical Engineering. Master.
Bo Zhang develops detection software of tool wear and does experiments of tool wear.

-Additional declarations for articles in life science journals that report the results of studies involving humans and/or animals
Not applicable

-Ethics approval (include appropriate approvals or waivers)
Not applicable

-Consent to participate (include appropriate statements)
Not applicable

-Consent for publication (include appropriate statements)
Written informed consent for publication was obtained from all participants.

Reference

[1] H. S, H. LW, X. MZ. (2004) A cutting power model for tool wear monitoring in milling. International Journal of Machine Tools and Manufacture,44.

[2] S. NH, K. KT, Y. SW, C. WDS, H. LG, W. WT. (2006) Tool wear detection and fault diagnosis based on cutting force monitoring. International Journal of Machine Tools and Manufacture,47

[3] Martín PG, Alfredo MH, José ER, Carlos EDA. (2010) Tool wear evaluation in drilling by acoustic emission. Physics Procedia,3.

[4] Mohammad M, Simon SP, Martin BGJ. (2009) Tool wear monitoring of micro-milling operations. Journal of Materials Processing Tech.,209.

[5] Wen-Yuh J, Tung-Hsien H, Po-Yu C, Ming-Shi W, Yu-Tso L. (2019) Evaluation of tool scraping wear conditions by image pattern recognition system. The International Journal of Advanced Manufacturing Technology,105.

[6] Peipei Z, Kesheng W, Qianhong H. (2017) Design of experiment based on tool wear condition by chip monitoring. Experimental Technology And Management,34:58-61(in Chinese).

[7] Shengqi G, Benben H, Hong L, Lizhong W. (2018) Tool Wear Detection using Gauss Fillter Saliency. Mechanical Science and Technology for Aerospace Engineering,37:276-279(in Chinese).

[8] Ruitao P, Haojian J, Ying X, Xianzi T, Shan Z. (2019) Study on Tool Wear Monitoring using Machine Vision. Mechanical Science and Technology for Aerospace Engineering,38:1257-1263(in Chinese).

[9] Guo-hua Q, Xin Y, Yi-ran L, Wen-bin X. (2014) Automatic detection technology and system for tool wear. Optics and Precision Engineering,22:3332-3341(in Chinese).

[10] Yu-song L, Jiang H. (2015) Application of image denoising method based on pixel-distribution on tool wear deteciton. Journal OF Machine Design,32:93-98(in Chinese).

[11] Shengqi G, Yunxian Q, Zhaoyuan G. (2013) A Tool Wear Detection by Wavelet Homomorphism Filtering. Mechanical Science and Technology for Aerospace Engineering,32:1703-1707(in Chinese).

[12] Jilin Z, Chen Z, Song G, Laishui Z. (2012) Research on tool wear detection based on machine vision in end milling process. Production Engineering,6.

[13] Zhang G, To S. (2017) Relation between tool wear and workpiece modal vibration in ultra-precision raster fly cutting. International journal of advanced manufacturing technology,93:3505-3515.

[14] Loizou J, Tian W, Robertson J, Camelio J. (2015) Automated wear characterization for broaching tools based on machine vision systems. Journal of manufacturing systems,37:558-563.

[15] LIU R. (2008) Research on cutting tool flank wear monitoring based on computer vision. Dissertation, Xi'an University Of Technology(in Chinese).

[16] Miaomiao Z. (2018) Rearch on End Mill Wear Detection Based on Machine Vision. Dissertation, Northwestern Polytechnical University(in Chinese).

[17] Yu-zhen H, Guo-qiang R, Jian S. (2014) Analysis and improvement on sharpness evaluation function of defocused image. Optics and Precision Engineering,22:3401-3408(in Chinese).

[18] ZHANG X. (2019) Filtering Algorithm Based on Gaussian-salt and Pepper Noise. Computer Science,46:263-265(in Chinese).

[19] Zhi-jia L, Yin-hui X, De-zhen Y, Yu L, Chang-bin. (2019) An improved method for infrared image noise processing based on median filter. Laser and Infrared | Laser Infr,49:376-380(in Chinese).

[20] F J, Q G, HZ H, N L, YW G, DX C. (2017) Survey on content-based image segmentation methods.

Journal of Software,28:160-183.

[21] Gao W, Shen-liang Y, Zhi-yong J, Su-ping M. (2019) An Improved Grabcut Algorithm for Color Images Segmentation. Software Guide,18:171-175(in Chinese).

[22] Guangfu L, He Z, Kaidi Z, Jixin J, Yunfei C. (2018) Study on the Quality Evaluation of Electric Submersible Pumps Based on Improved K-means. Journal of Southwest Petroleum University（Science & Technology Edition）,40:173-180(in Chinese).

[23] Dong-kai T, Hong-mei W, Ming H, Gang L. (2018) Optimizing Initial Cluster Center of Improved K-means Algorithm. Journal of Chinese Mini-Micro Computer Systems | J Chin Mini-Micro Comput Syst,39:1819-1823(in Chinese).

[24] Bo Z. (2019) Research on Tool Wear Detection Method of Lathe Based on Machine Vision. Dissertation, Wuhan University of Technology(in Chinese).

[25] Zhaojun L, Jun Z. (2019) Adaptive Canny algorithm improved based on Otsu algorithm and histogram. Modern Electronics Technique,42:54-58(in Chinese).

[26] Yan D, Chenke W, Hua L, Bijiao W. (2018) Line Detection Optimization Algorithm Based on Improved Probabilistic Hough Transform. Acta Optica Sinica | Acta Optic Sin,38:170-178(in Chinese).

Figures

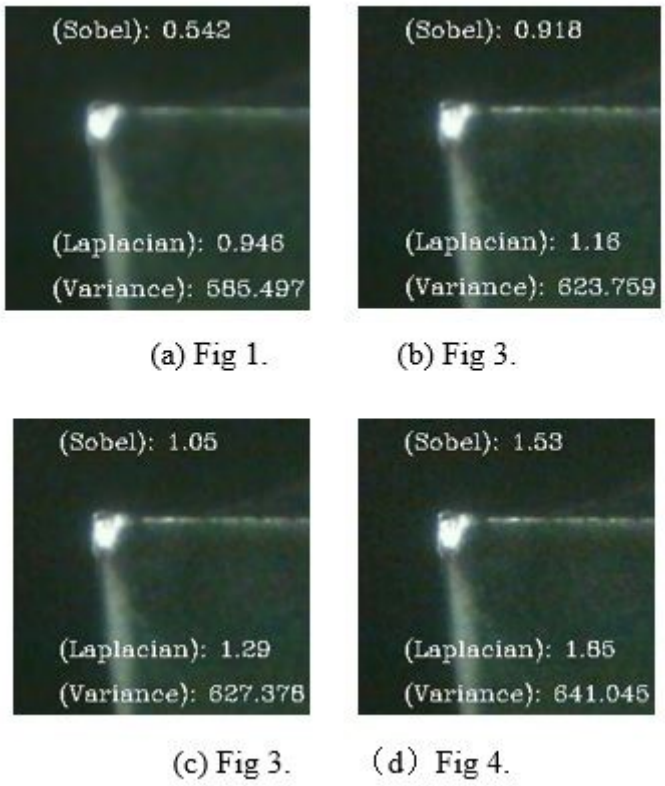

Figure 1

2-1 Evaluation results using sharpness evaluation function

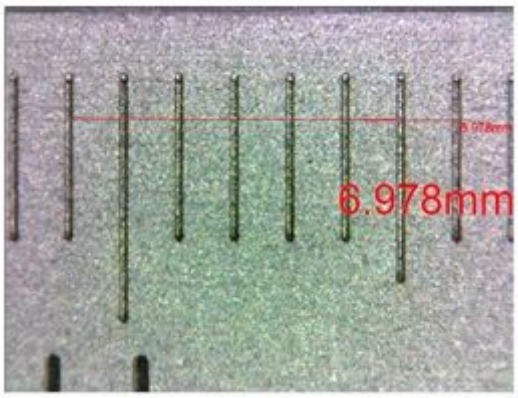

Figure 2

2-2 Image taken by camera

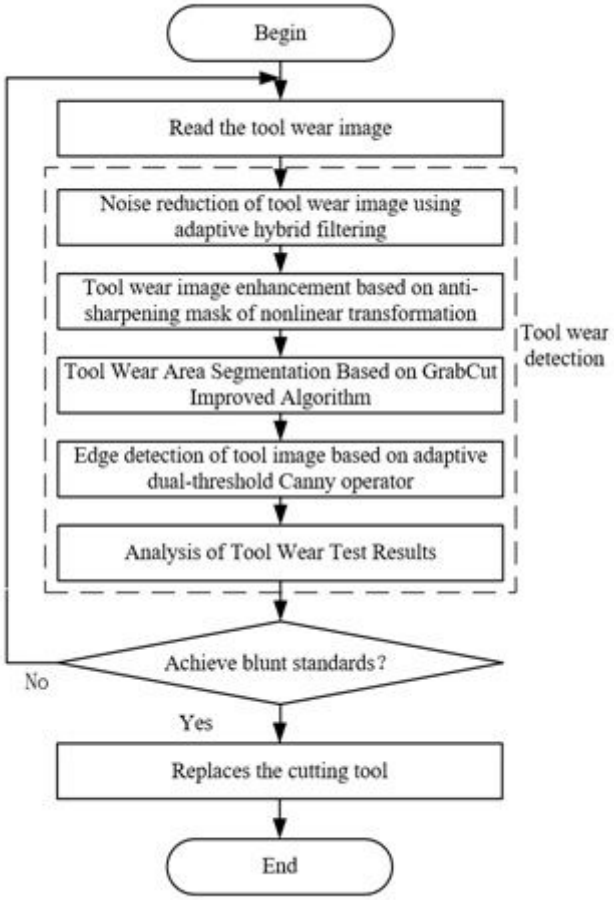

Figure 3

3-1 Tool wear image processing flow chart

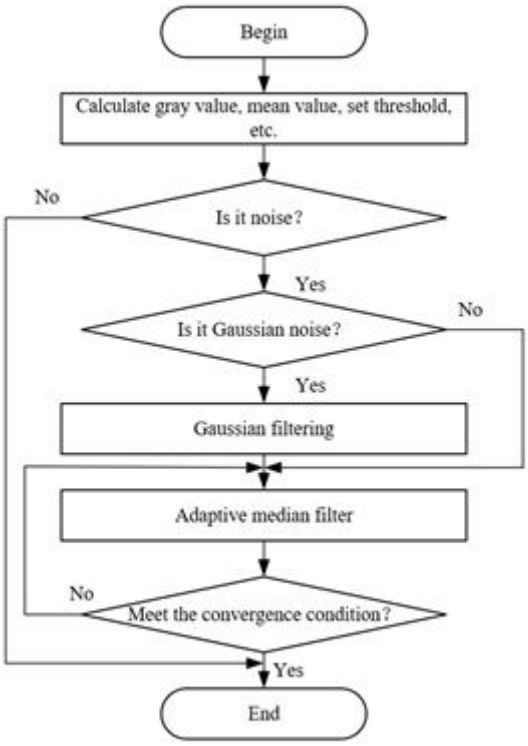

Figure 4

3-2 Adaptive hybrid filtering process flow chart

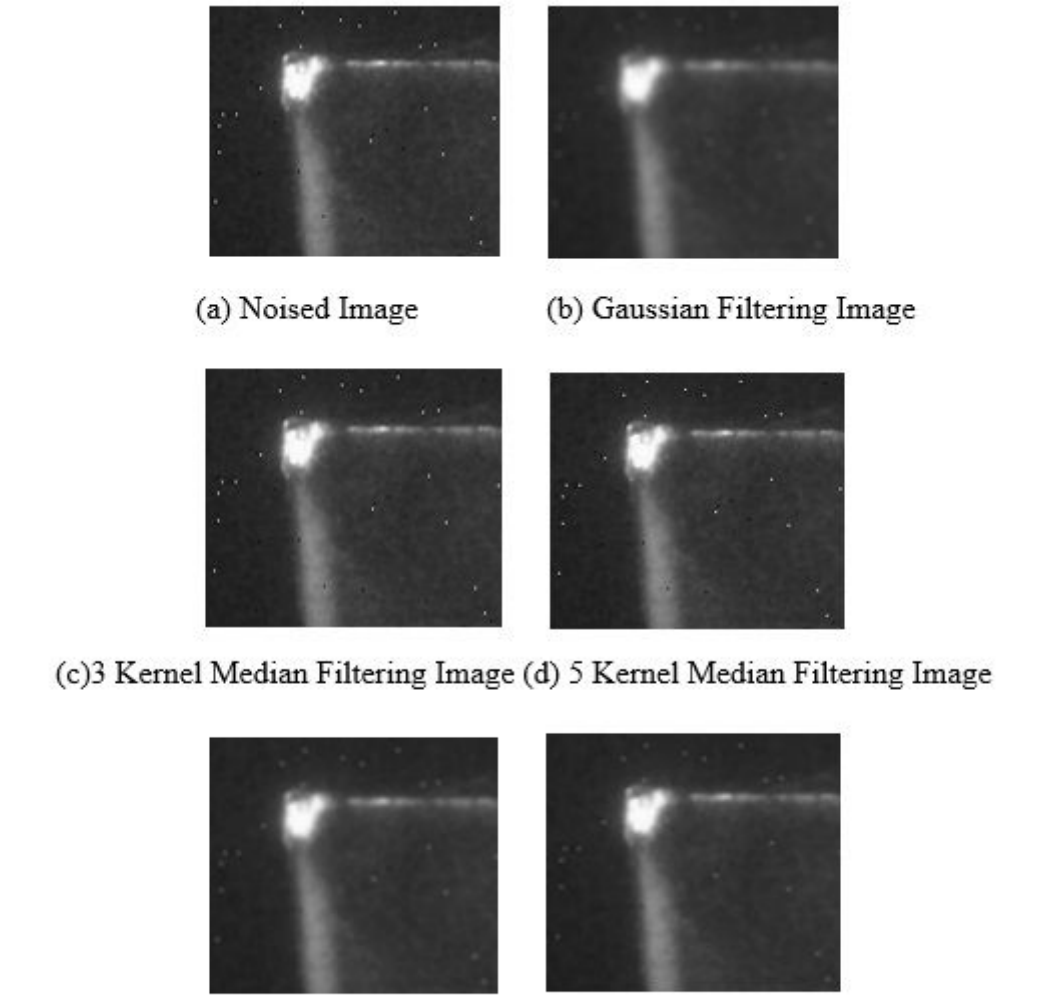

Figure 5

3-3 Comparison of Gaussian Filtering, Median Filtering, and Adaptive Hybrid Filtering

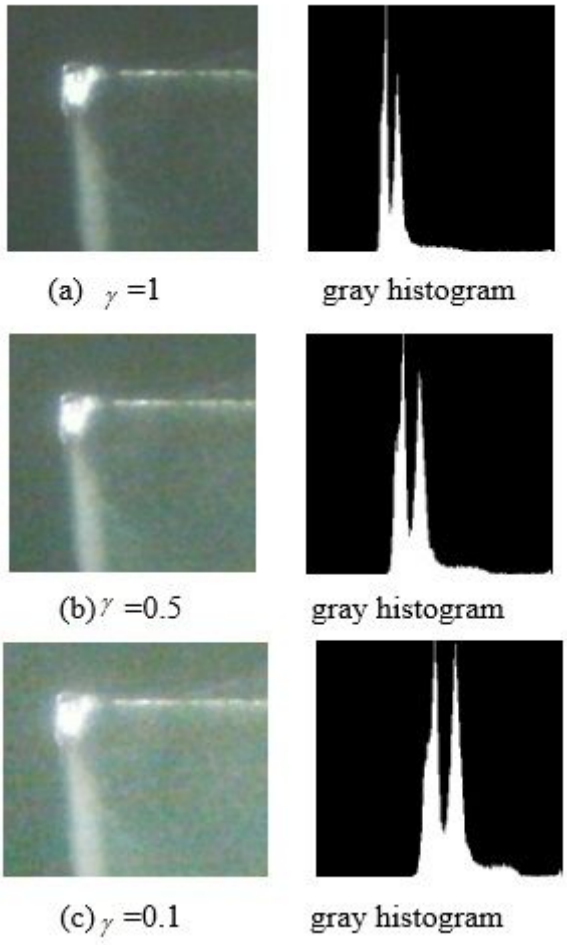

Figure 6

3-4 Images and corresponding gray histograms under different Gamma correction coefficients

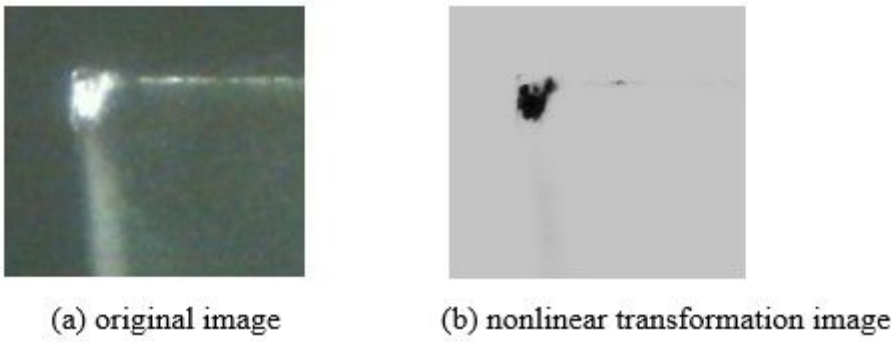

Figure 7

3-5 Original image and results of image suppression after nonlinear transformation

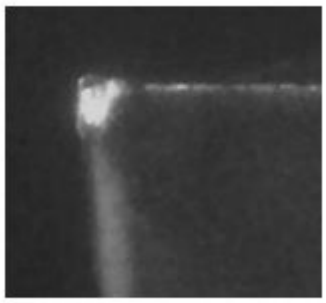

Figure 8

3-6 Gamma correction, nonlinear transformation and original image synthesis results

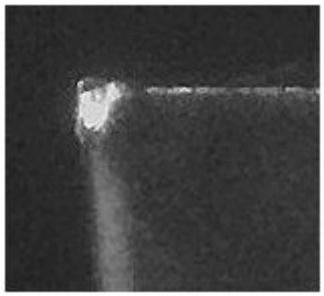

Figure 9

3-7 Result image processed by anti-sharp masking algorithm

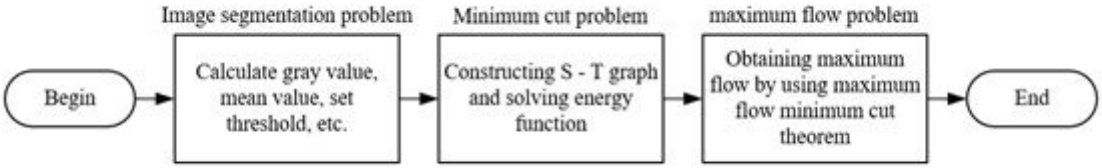

Figure 10

3-8 The process of image segmentation by GrabCut algorithm

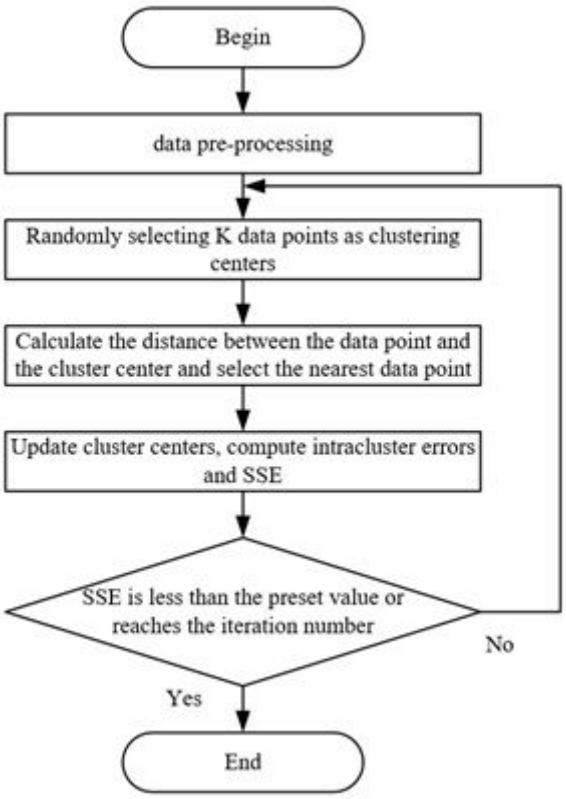

Figure 11

3-9 The basic process of K-means clustering algorithm

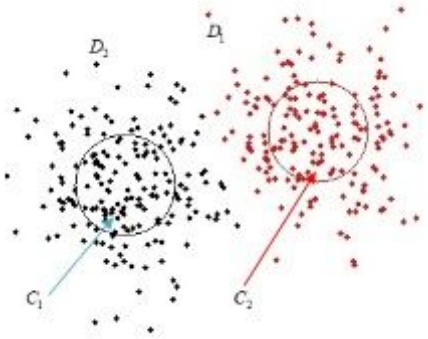

Figure 12

3-10 Clusters and isolated points

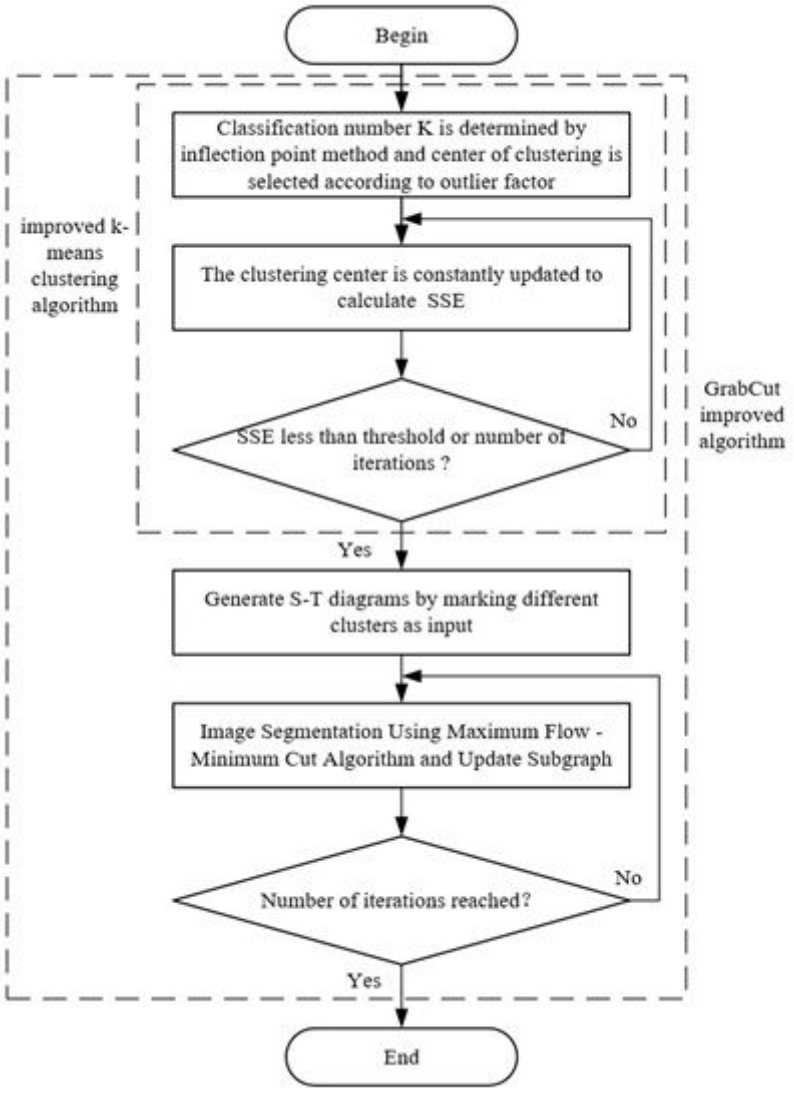

Figure 13

3-11 Image segmentation process based on GrabCut improved algorithm

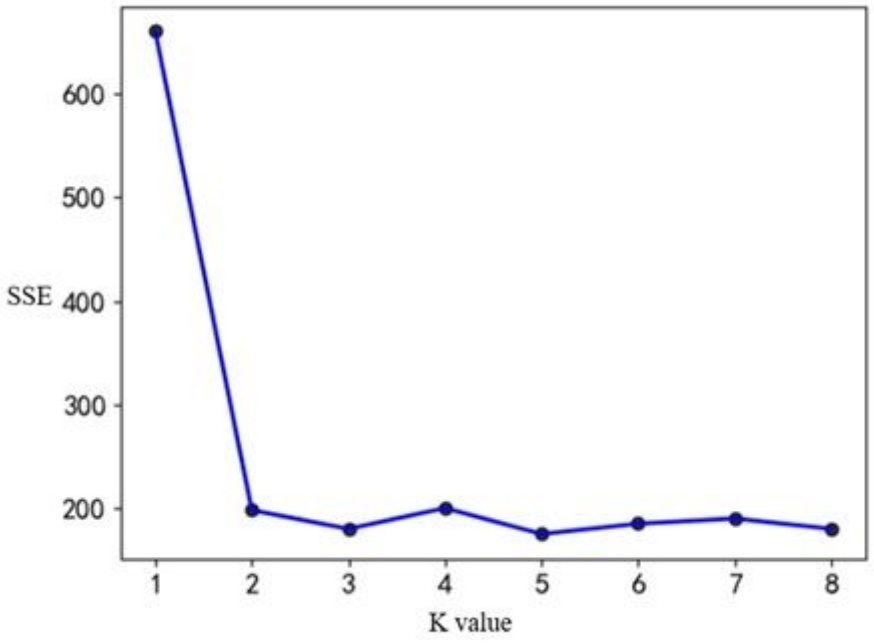

Figure 14

3-12 The relationship between value and SSE

Figure 15

3-13 Traditional GrabCut segmentation result

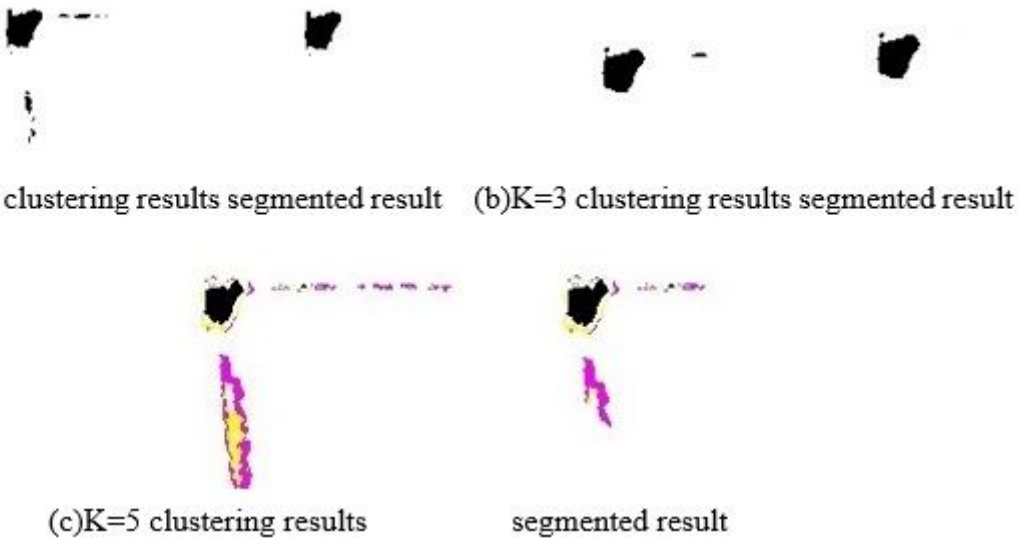

(a)K=2 clustering results segmented result (b)K=3 clustering results segmented result

(c)K=5 clustering results segmented result

Figure 16

3-14 Segmentation results of GrabCut improved algorithm

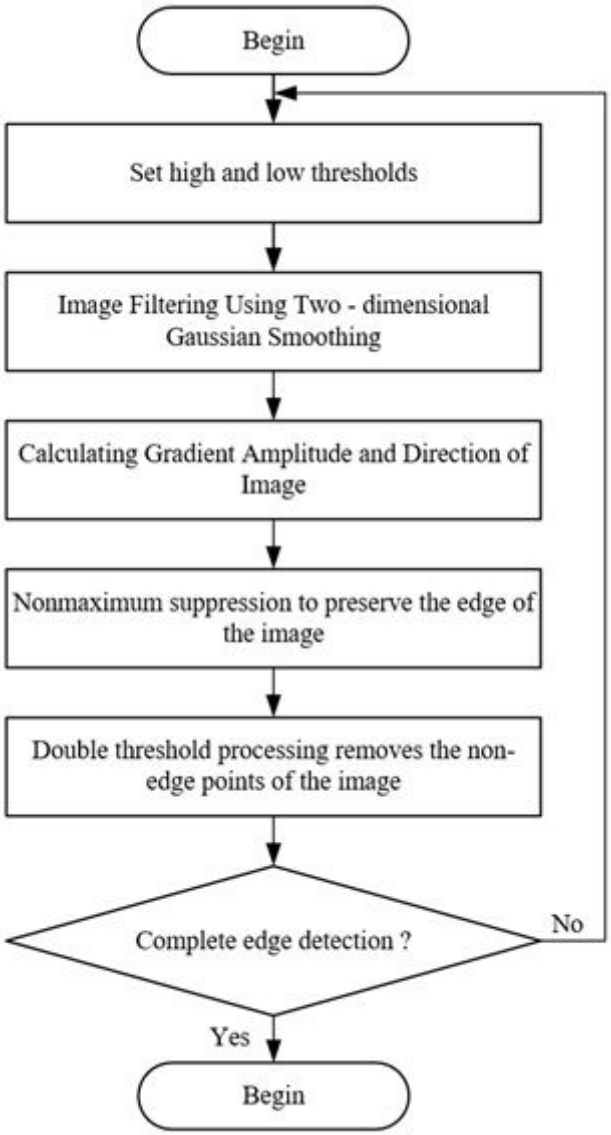

Figure 17

3-16 Canny edge detection process flow chart

(a) Canny edge detector (b) Sobel algorithm (c) Laplace operator (d) Canny operator adapting to double thresholds

Figure 18

3-17 Comparison of edge detection operator results

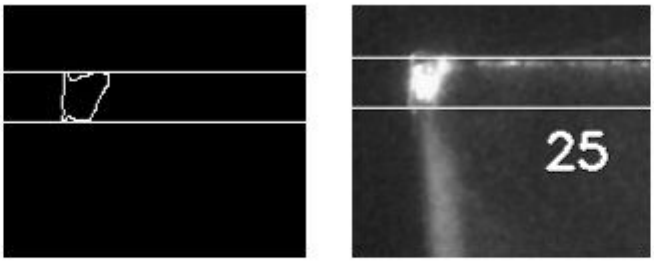

(a) Hough transform results (b) The upper and lower boundaries pixel values of the wear region

Figure 19

3-20 Hough transform detection results Tool wear detection experiment and analysis

(a) Lathe machine

(b) Image acquisition system

(c) Software Measuring Interface of Computer

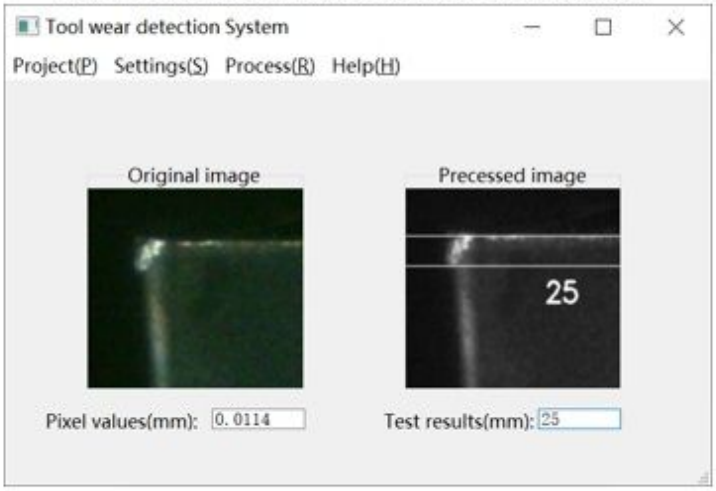

(d) Software interface

Figure 20

4-1 Tool wear detection system